On the usage of the effectively shaped indenter concept for analysis of yield strength

M. Herrmann[a] and F. Richter
Chemnitz University of Technology, Institute of Physics, 09107 Chemnitz, Germany

(Received 18 August 2008; accepted 8 December 2008)

Using the extended Hertzian approach (EHA), the "effectively shaped indenter" corresponding to Pharr's concept is described in terms of a parameter set $\{d_0,d_2,d_4,d_6\}$, which can be determined by a fitting procedure from the unloading curve of an indentation experiment. Owing to the limited accuracy of measurement, a given experimental curve may in principle correspond to more than one such parameter set. Based on indentation experiments with a Berkovich indenter into fused silica, we have investigated the influence of the fitting procedure itself on the results. We suggest a certain manual fitting procedure, which delivered a yield strength $Y = (7.1 \pm 0.1)$ GPa independent of the maximum load. Manual fitting always includes some degree of subjectivity, however, both Y and the elastic field as a whole proved to be relatively robust against modifications of the parameter set. We also suggest a preliminary objective procedure, which delivered $Y = 6.8 - 7.1$ GPa. In addition, we have performed finite element method (FEM) simulations of elastic–plastic indentations of a conical indenter into a von Mises solid with a yield strength of $Y = 7.0$ GPa. The simulated unloading curve was analyzed using the EHA in the same manner as the experimental curves, and yield strength of 6.95 GPa was obtained being very close to the input value of the FEM.

I. INTRODUCTION

Nanoindentation at submicron scale as a suitable technique to measure mechanical properties of materials has been established over the last decade. In particular, this method has been widely adopted to determine Young's modulus and hardness of bulk materials and thin films. A major step in the understanding of the indentation response of materials has been brought about by the introduction of the concept of the "effectively shaped indenter" by Pharr and Bolshakov.[1,2] In this concept, the real indenter penetrating into the plastically deformed hardness impression is substituted by an imaginary so-called "effectively shaped indenter," which delivers the same unloading curve when penetrating into a flat elastic half space. The shape of the "effective indenter" is derived from the inspection of the unloading curve, which is assumed to be wholly elastic. With this approach, the theoretical treatment of nanoindentation was enormously extended, so that elastic–plastic contact situations—the most likely situation in the case of sharp indenter tips—can be assessed on the basis of a linear-elastic contact theory. Oliver and Pharr[1] were able to derive the normal displacement and the contact pressure distribution at the surface due to the acting effective indenter by using the results of Sneddon.[3] Later, this approach was extended in the form of Schwarzer's extended Hertzian approach (EHA), which made it possible to compute the complete elastic stress and strain fields within the indented body.[4,5] Moreover, Schwarzer transferred this approach to layered bodies with the help of his so-called method of the Image Loads.[6] With the known elastic fields, Young's modulus can be calculated.[4] Furthermore, certain stress components or combinations of stress components can be determined that are related to the onset of a particular failure mode. For instance, the radial tensile stresses shall be mentioned here, which can lead to the formation of cracks like Hertzian cone cracks or star cracks. In addition the combination of stress components, according to the von Mises stress formula (compare Sec. II. D), is correlated to the onset of plastic flow within the material.

An important variant of data evaluation is to determine the shape of the effective indenter in terms of the parameters d_0, d_2, d_4, and d_6 corresponding to the governing contact equation of the EHA [compare Sec. II. C, Eq. (13)] from the unloading curve and then to use it to calculate the elastic von Mises stress distribution at the moment of beginning unloading at maximum load. This stage represents, at the same time, the last point of the loading curve at which plastic deformation took place during loading and where an infinitesimal increase of the load would immediately cause plastic deformation

[a]Address all correspondence to this author.
e-mail: matthias.herrmann@physik.tu-chemnitz.de
DOI: 10.1557/JMR.2009.0125

to start again. In view of this fact, it is considered possible to determine the yield strength in the form of the spatial maximum of the elastic von Mises stress distribution at maximum load, thus getting information on plastic deformation from an elastic theory. Indeed, it could be shown for several bulk and thin film samples that this approach applied to unloading curves obtained by Berkovich indenters is capable to deliver reliable yield strength values.[4,7]

In this work, the problem shall be investigated that—owing to the limited accuracy of measurement—the effectively shaped indenter following from a certain unloading curve may in principle be described by more than one parameter set $\{d_0,d_2,d_4,d_6\}$. This could cause considerations of whether the existence of several equivalent parameter sets could produce different values for the quantities of interest like yield strength or Young's modulus, thus preventing definite results.

The work is based on indentation studies using a Berkovich indenter on fused silica together with finite element method (FEM) simulations. First, the influence of a varying maximum load on the experimentally determined hardness and yield strength values was investigated, putting special emphasis on the influence of the fitting procedure itself on the yield strength results. Second, load–depth curves were simulated by FEM for an equivalent cone of the same angle as for the Berkovich indenter. For this simulation, a material constitutive equation using Young's modulus and yield strength of fused silica was applied. Then, the yield strength was determined by analysis of the simulated elastic–plastic load–depth curve by using the concept of the effectively shaped indenter and the resulting value was compared to the yield strength used as an input parameter to the FEM simulations.

We begin by presenting some basics of nanoindentation analysis, particularly, the Oliver–Pharr method and their relations to the concept of the effectively shaped indenter. Moreover, in Sec. II, the concept of the effectively shaped indenter and its use by means of the EHA is presented with respect to the determination of yield strength. Section III is dedicated to the experimental studies at varying maximum loads and the determination of hardness and yield strength. In Sec. IV the FEM simulation is presented together with its results. Finally, the resulting contact pressure and elastic von Mises stress distributions due to the effective indenter are given for the experimental as well as the FEM study.

II. CONCEPT OF THE EFFECTIVELY SHAPED INDENTER

A. Basics of nanoindentation

In recent years numerous methods have been developed for measuring the mechanical properties of materials by means of load- and depth-sensing indentation testing. One of the commonly used methods for analyzing nanoindentation load–depth data is that of Oliver and Pharr.[8] They generalized the approach used by Loubet et al.[9] and Doerner and Nix,[10] which was constrained by the assumption of a flat punch indenter geometry. The method was developed to determine hardness and Young's modulus of a material from load–depth data obtained during one complete cycle of loading and unloading. During this cycle, the load, P, and the indentation depth, h, which is defined as the displacement relative to the initial underformed surface, are simultaneously monitored. The deformation during loading is assumed to be both elastic and plastic, while the recovery of the material during unloading is considered to be purely elastic. In fact, the elastic character of the recovery during unloading is the basic assumption in the analysis. Hence, this method cannot be used for materials that, for instance, show reverse plasticity.

The analysis starts by fitting the unloading curve with the help of a power-law relation

$$P = \alpha(h - h_f)^m \quad , \tag{1}$$

where α and m are fitting parameters, which are empirically determined, and h_f is the final depth after full unloading. Experiments with a Berkovich indenter on a wide variety of materials have shown that the power law exponent m ranges from $1.2 \leq m \leq 1.6$.[1] These results are close to the value for a paraboloid of revolution ($m = 1.5$) but different to both the value of a flat punch having $m = 1$ and a conical indenter with $m = 2$. The reader should keep in mind that the latter represents the axisymmetric equivalent of a pyramidal Berkovich indenter. For further analysis, it is assumed that the contact periphery is situated because of elastic deformation by distance h_s below the original sample surface. The elastic models deliver that h_s follows with

$$h_s = \epsilon P_{max}/S \quad , \tag{2}$$

where ϵ is a constant that depends on the indenter geometry. It has been found that $\epsilon = 0.75$ for a paraboloid of revolution, $\epsilon = 1$ for a flat punch geometry, and $\epsilon = 0.72$ for a conical punch. The parameter P_{max} is the maximum indentation load, and S is the contact stiffness, the slope of the upper part of the unloading curve during the initial stages of unloading.

From the contact geometry, it follows that the depth h_c, where the indenter and the specimen are in contact, is given by[3]

$$h_c = h_{max} - h_s = h_{max} - \epsilon P_{max}/S \quad . \tag{3}$$

The contact stiffness is obtained by differentiating Eq. (1) at the maximum depth of indentation, where $h = h_{max}$, giving

$$S = dP/dh(h = h_{max}) = m\alpha(h_{max} - h_f)^{m-1} \quad . \quad (4)$$

From these measurements, the contact area of the indenter, A, can be related to the contact depth in the form of an indenter shape function or area function $A = f(h_c)$. With known contact area, the hardness of the specimen is derived from

$$H = P_{max}/A \quad . \quad (5)$$

The Young's modulus, E, is determined from the relation of the contact area to the contact stiffness given by

$$E_{red} = \frac{1}{\beta}\frac{\pi^{1/2}}{2}\frac{S}{A^{1/2}} \quad , \quad (6)$$

where the reduced modulus E_{red} is defined as

$$\frac{1}{E_{red}} = \frac{1-\nu_i^2}{E_i} + \frac{1-\nu^2}{E} \quad . \quad (7)$$

The reduced modulus is used to describe that elastic displacements occur in both the specimen and the indenter. Here, E and ν are Young's modulus and Poisson's ratio for the specimen; E_i and ν_i are the same quantities for the indenter.

The factor β in Eq. (6) serves as a correction that depends on the half-included angle of the indenter, and Poisson's ratio of the indented material. Eq. (6) is based on the elastic contact theory for indentation into an elastic half-space, which was developed by Sneddon.[3] Using the results of Sneddon's analysis a radial surface displacement for the indentation of rigid cone into an elastic half-space would be obtained, which is not consistent with the deformation by a rigid cone. The necessity to correct the load and contact stiffness to provide accurate hardness and Young's modulus from indentation data led to the development of some analytical approximations for β, which are simple modifications to Sneddon's solution. For a detailed discussion see Hay et al.[11] Finally, with this correction, an accurate determination of hardness and Young's modulus of a bulk specimen is obtained from indentation load–depth data for indenters having axisymmetric shape.

B. Concept of the effectively shaped indenter

As previously mentioned in Sec. II. A, unloading curves obtained with Berkovich indenters are usually well described by a power-law relation according to Eq. (1) with an exponent in the range $1.2 \leq m \leq 1.6$. This is different than the value given due to the elastic contact by the conical indenter ($m = 2$) indicating that the pressure distribution under the indenter is influenced by the plasticity during indentation. An introduction to this problem was given by Woirgard and Dargenton[12] as well as by Pharr and Bolshakov.[1] A comprehensive investigation of the effectively shaped indenter concept and its use for the analysis of nanoindentation data have been conducted by Oliver and Pharr.[2]

During elastic unloading the contact area is continuously decreased, from full contact at maximum load until zero. This causes a continuous decrease of the slope of the unloading curve. The maximum value of the slope exists at maximum load and is referred to as (initial) elastic unloading stiffness, S:

$$S = \frac{dP}{dh} = \beta\frac{2}{\pi^{1/2}}E_{eff}A^{1/2} \quad . \quad (8)$$

Now, the effectively shaped indenter concept comes into play, which accounts for the fact that the contact is not between a conical indenter and a flat elastic half-space, but a conical indenter pressed into the surface that has been distorted by the formation of the residual impression. The basic idea is to change the shape of the indenter to an effective shape so that the same normal surface displacement on a flat surface is produced that would be produced by the conical indenter on the deformed surface. Therefore, the surface distortion is accounted for by the transformed contact geometry into one which allows the application of elastic half-space solutions. The shape of the effectively shaped indenter may be approximated by the power-law function

$$z = u(r) \cong B \cdot r^n \quad , \quad (9)$$

where $u(r)$ is the distance between the conical indenter and the surface of the unloaded residual impression, r is the radial coordinate, B is a fitting constant, and n ranges from 2 to 6 for a variety of materials. For the deformation of an elastic half-space by a rigid indenter of a shape corresponding to Eq. (9), Sneddon's analysis delivered

$$P = \frac{2E_{eff}}{(\pi^{1/2}B)}^{1/n}\left(\frac{n}{n+1}\right)\left[\frac{\Gamma(n/2+1/2)}{\Gamma(n/2+1)}\right]^{1/n}h^{1+1/n} \quad , \quad (10)$$

where h is the elastic displacement, and Γ is the gamma function. The exponent n in Eq. (9) and Eq. (10), which describes the shape of the effectively shaped indenter, is directly related to the exponent m in Eq. (1) describing the shape of the unloading curve. The comparison of Eq. (1) and Eq. (10) delivers

$$m = 1 + 1/n \quad , \quad (11)$$

which gives m-values in the range 1.2–1.6 for n-values from 2 to 6. Thus, the parabolic shape of the effectively shaped indenter represents an explanation for the fact that the unloading behavior is similar to that of a paraboloid of revolution ($m \approx 1.5$) rather than that of a cone.

C. Concept of the effectively shaped indenter treated by the extended Hertzian approach

Since the introduction of the theory of the linear elastic contact of two parabolic bodies by Hertz,[13,14]

several authors have attempted to complete his solution, which was limited to some components of stress and normal displacement. A very compact closed form solution of the Hertzian contact problem was given by Hanson for the isotropic and transverse isotropic case, where the mathematical basis was introduced by Fabrikant.[15] The next step was the extension of the solution to layered media, where a detailed discussion is provided by Schwarzer.[6] He applied a method called Image Load Method (ILM) to obtain the complete elastic fields within the layered specimen. His elastic solution was successfully used for nanoindentation analysis; for example, the determination of Young's modulus of thin and very thin films,[16–19] investigation of load-carrying capacity of thin film structures,[20–22] or yield strength analysis of thin films.[20,23] Schwarzer's approach was basically restricted due to the Hertzian contact formulation to surface displacements of the parabolic shape of the indenting body w_i and specimen w_s with

$$w_i(r) + w_s(r) = h - r^2/d_0 \quad , \tag{12}$$

where r is the radial coordinate and d_0 is a quantity describing the curvature of the contacting bodies. In case of the contact of a rigid sphere of radius R with a half-space, the quantity d_0 is related to the spherical radius by $d_0 = 2\,R$, and the spherical radius is exactly the radius of curvature of the deformed surface of the half-space under the indenter. Pharr's work on the concept of the effectively shaped indenter, as previously mentioned in Sec. II, used a Sneddon approach, which is restricted to surface information in terms of the normal displacement and surface pressure, because the Hertzian theory was restricted to the parabolic shape of the surface given by Eq. (12). Therefore, the complete elastic fields within the specimen due to the effectively shaped indenter could not be gained from the Sneddon approach. To overcome these restrictions, Schwarzer extended the Hertzian theory establishing the so-called EHA and evaluated the complete potentials for the elastic field due to a governing contact equation of the type[4]

$$w_i(r)+w_s(r)=h-r^2/d_0-r^4/d_2-r^6/d_4-r^8/d_6 \ . \tag{13}$$

The corresponding surface normal pressure distributions are given of the form

$$\sigma_{zz}(0 \le r \le a, z = 0) = \sum_{n=0}^{N} c_n r^n (a^2 - r^2)^{1/2} \quad , \tag{14}$$

where the c_n are arbitrary constants following from the complete potentials and n are even exponents.[4] This contact formulation together with the ILM allows evaluating the shape of the effective indenter and the corresponding resulting surface pressure distribution as well as the complete elastic stress field also within the layered specimen. The detailed mathematical procedure is given elsewhere.[4,24] From the known shape of the effective indenter in terms of the d_i coefficients in Eq. (13), the resulting surface pressure distribution according to Eq. (14) is obtained, which then delivers the complete elastic stress, strain, and deformation fields within the specimen when all experimental boundary conditions are considered properly (e.g., film thickness, elastic properties of specimen). It should be emphasized that the elastic field mentioned here is the field produced by the imaginary effectively shaped indenter within a flat body. However, owing to the definition of the effectively shaped indenter this field is equal to the field formed by the real pointed indenter acting elastically on the plastically deformed surface of the real sample. The same is true for the contact pressure distribution (It should be pointed out that the contact pressure between real indenter and sample mentioned here is for the elastic case, i.e., it holds for the gedanken experiment. It must not be mixed up with the contact pressure during the elastic–plastic indentation of a pointed indenter.) in those two cases. Thus, the concept of the effectively shaped indenter corresponds to a gedanken experiment where the real indenter is reindented into the surface depression following the elastic unloading curve but in opposite direction. This approach permits us to investigate elastic behavior as well as the onset of plastic deformation.

A main limitation of the concept consists of the condition that the stresses due to the indenter must be dominated by the elastic contribution and that the influence of the residual stresses due to inelastic deformation is small (for a detailed explanation see Ref. 23). The fused silica investigated in this work is particularly well suited to be treated by the method. For other materials that show, e.g., work hardening and/or have a large E/Y ratio, the methodology may be ineffective. However, to define the limits of applicability of the effectively shaped indenter concept in terms of the stress–strain behavior of the material is a task that still has to be done in future.

D. Concept of the effectively shaped indenter applied for the determination of yield strength

To describe the onset of plastic deformation we make use of the von Mises criterion. This criterion means that if the so-called von Mises stress in a material exceeds a certain material-specific limit, plastic flow occurs. The elastic von Mises stress is defined by

$$2\sigma_M^2 = (\sigma_{xx} - \sigma_{yy})^2 + (\sigma_{yy} - \sigma_{zz})^2 + (\sigma_{zz} - \sigma_{xx})^2 + 6(\tau_{xy}^2 + \tau_{yz}^2 + \tau_{zx}^2) \quad , \tag{15}$$

where σ_{xx}, σ_{yy}, σ_{zz}, τ_{xy}, τ_{yz}, and τ_{zx} are the normal and shearing stresses in Cartesian coordinates. This stress equals the octahedral shear stress multiplied by a factor of $3/2^{1/2}$, which makes sure that the von Mises stress and

the yield strength obtained by the uniaxial tensile test have the same value. Therefore, provided that yielding occurs, the spatial maximum of the elastic von Mises stress distribution should be equal to the yield strength.

If an elastic theory is used for the determination of the von Mises stress distribution, one has to keep in mind that the elastic calculation is only valid as long as no plastic deformation takes place. In the case of a purely elastic stress state the calculation will be correct; however, the von Mises stress will be smaller than the yield strength everywhere in the sample and will not deliver information about yielding. It is only for the very moment of the onset of plastic deformation that the spatial maximum of the elastic von Mises stress distribution equals the yield strength. This approach is applied in the loading-partial unloading method where a spherical indenter is gradually pressed into the sample, and the moment of the onset of plastic deformation monitored.[20] For that state, the elastic theory can still be used and delivers the yield strength in the form of the spatial maximum of the elastic von Mises stress. This method has successfully been used for the determination of yield strength by spherical indentation for both bulk[25] and thin film samples.[20]

The effectively shaped indenter is also accessible to this kind of approach. As mentioned in Sec. II. C, the concept of the effectively shaped indenter can be used to evaluate a gedanken experiment where the real indenter is indented into the surface depression formed previously. In terms of the load–displacement curve this gedanken experiment corresponds to the movement of the indenter along the unloading curve but in opposite direction. This is to a large extent analogue to the general approach mentioned previously because this process is completely elastic and is evaluated up to the original point of maximum indentation, where an infinitesimal further increase causes plastic deformation to start again. At maximum load the elastic field formed by the real pointed indenter acting on the real sample is still equal to the field produced by the effectively shaped indenter within a flat body. Using the EHA the latter can be calculated, including the distribution of the elastic von Mises stress whose spatial maximum is equal to the yield strength of the material.

The experimental procedure includes an elastic–plastic loading experiment using a pointed indenter followed by unloading. From the upper part of the unloading curve the shape of the effective indenter, related to the maximum load, is derived and used for the calculation mentioned previously.

III. APPLICATION OF THE EFFECTIVE INDENTER CONCEPT TO EXPERIMENTAL DATA

A. Nanoindentation experiments

The measurements were carried out with a UMIS-2000 nanoindenter (CSIRO, Australia) equipped with a Berkovich indenter made of diamond. The device has a depth resolution of about 0.1 nm and a force resolution of about 0.75 μN. The real indenter shape in the form of an area function and the instrument stiffness function were determined by means of reference measurements in sapphire and fused silica. Measurements with varying maximum loads (P_{max} = 3, 10, 50 mN) were carried out on every sample, where each of them was repeated 10 times. The single load–depth curves at each load were averaged to ensure reasonable statistics. The standard measurement cycle consists of five periods with surface detection, increase of load up to the maximum, hold period at constant load to reduce creep effects, unload to about 0.10-P_{max}, and second hold period at that load for thermal drift correction. To detect the zero position of the measurement curve, the data points of the first part of the curve were fitted using the load–depth relation $P = \text{const.}(h-h_0)^{1.5}$ (with h_0 as zero shift) for an elastic contact of a sphere on a flat surface. This approach can be used to correct the load–depth data also in the case of Berkovich indentation because the pointed indenters always show a certain tip rounding. Thus, the first part of the load–displacement curve can be well approximated by an elastic contact. A least-square fit is used to find the best agreement between measurement data and fit. For the hold period at maximum load a duration of 20 s was chosen, which was found to be best suited to reduce the influence of creep effects. At the second hold period mentioned previously, the depth was monitored at constant load during a time period of 45 s. The first quarter of this period was not used for a further correction because it may be influenced by relaxation processes within the material. A linear fit was then applied to the remaining data, which delivered a drift rate in nm/s. This thermal drift rate was then used to correct the complete load–depth data of the cycle.

Finally, the Young's modulus and hardness of the sample were analyzed using a modified Oliver–Pharr method,[26] where a value of $\nu = 0.17$ for the Poisson's ratio of the sample were used. The modification implements a correction concerning the radial displacement as a function of the ratio H/E and a variable E factor [compare Eq. (3)]. Then, the unloading part of the experimental load–depth curves were fitted to determine the shape of the effective indenter by means of the EHA, according to Sec. II. C. Additionally, the unloading exponent m of the unloading curve was analyzed according to Eq. (1) for all measured loads.

B. Analysis of the load–depth curves

In Fig. 1, a load–depth curve, which is typically obtained for fused silica, is shown for a maximum load of 50 mN, as an example. The corresponding values of the maximum indentation depth and contact radius are

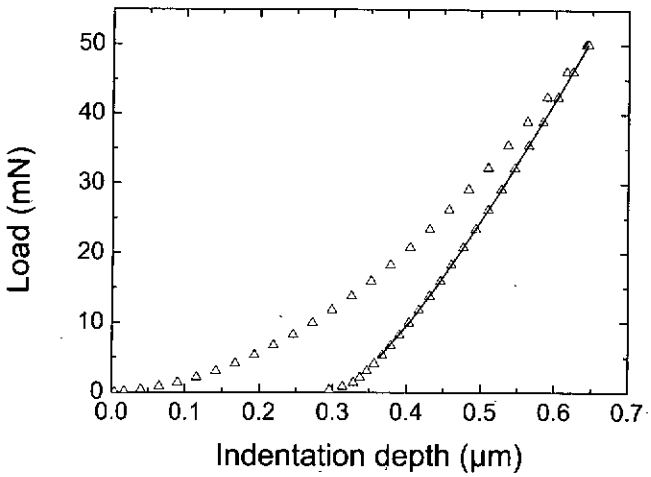

FIG. 1. Measured load–depth curve for fused silica at a maximum load of 50 mN, as an example. With the usage of the EHA, the d_i coefficients corresponding to Eq. (13) have been determined directly from the data points of the unloading curves to find the shape of the effective indenter (solid line).

given in Table I, where the latter one was calculated from the contact depth using the area function of the indenter (compare Sec. II. A).

The unloading curves could be well fitted by the power-law relation $P = \alpha\,(h - h_f)^m$ and deliver an unloading exponent of $m = 1.23$ for the load of 50 mN (compare Table I). The m-values for 3 and 10 mN, which are also given in Table I, proved that the unloading exponent remained constant at about 1.23 within the load range investigated. The indentation behavior was elastic–plastic for all three load–depth curves and allowed determining proper hardness values. The hardness values were in the range of $H = 8.2$–8.6 GPa depending on the maximum load (compare Table I). Young's modulus was derived from the same measuring data and delivered about 70 GPa, practically independent of the maximum load (Table I). Hence, both quantities can be considered to be constant within the error of measurement.

In a next step, with the usage of the EHA, the d_i coefficients corresponding to Eq. (13) have been determined directly from the data points of the unloading curves to find the shape of the effective indenter, which models the unloading curve (compare Fig. 1). Different procedures to determine the coefficients have been applied and all results are listed in Table II.

First, the measured unloading curves have been fitted manually. This was done by choosing tentative d_i coefficients and taking them for the generation of simulated curves corresponding to Eq. (13), using the software package FilmDoctor.[24] [Software for the evaluation of the elastic field of arbitrary combinations of normal and tangential loads of the type $\propto \sum_{n=0}^{N} c_n r^n (a^2 - r^2)^{1/2}$ (n = 0,2,4,6)]. The simulation of the unloading curves was performed in the following way. The governing contact equation [compare Eq. (13)] was solved for the selected set of d_i coefficients to satisfy all necessary boundary conditions and to find the contact radius; then, the elastic unloading curve was calculated for the given shape of the effective indenter. The degree of agreement between measured and simulated curves was assessed visually as well as using the deviation [root mean square (rms)] of the curves in the region from 100% down to 10% of maximum load. In a first step, d_0 was adjusted for best agreement of the curves. Then, d_2, d_4, and d_6 were varied one after another (in that sequence) to further improve the quality of the fit. In this manner, the fits for all three maximum loads were performed [data sets 3, 10, and 50 (a)], yielding similar maximum values of the elastic von Mises stress.

To investigate the influence of a variation of the set of d_i parameters on the maximum value of the elastic von Mises stress value obtained, d_0 was first modified by about 10% [from 22 to 24 μm, compare parameter set 50 (b)], and again the parameters d_2, d_4, and d_6 were varied one after another. An analogous procedure was performed for set 50 (c) where, however, d_0 was doubled. The latter simulation yielded a $d_6 = 3000$ μm^7, which delivered practically identical results as if d_6 would be set to infinite [compare parameter set 50 (d)]. We see from the data sets 3, 10, 50 (a), and 50 (b) that the yield strength is within (7.1 ± 0.1) GPa, independent of the maximum load. Provided that the parameters are varied one after another in the sequence d_0, d_2, d_4, d_6, slight deviations in the parameters as they normally occur by a manual fitting procedure have no significant influence. Even an intentional large variation of the most influential coefficient d_0 for parameters sets 50 (c) and 50 (d) yields only a negligible increase of the maximum value of the elastic von Mises stress from 7.1 to 7.2 GPa.

This—at first glance surprising—fact becomes clearer with Fig. 2, which shows the shapes of the five effectively shaped indenters, investigated for the maximum

TABLE I. Results of the load series for fused silica.

Load P (mN)	Maximum indentation depth h_{max} (μm)	Contact radius a (μm)	Unloading exponent m	Hardness H (GPa)	Young's modulus E (GPa)
3	0.1487	0.341	1.23	8.20	69.8
10	0.2808	0.609	1.22	8.59	70.4
50	0.6454	1.368	1.23	8.50	69.8

TABLE II. Overview of the d_i coefficients used for the fit of the shape of the effective indenter by means of the EHA.

Data set	Load P (mN)	d_0 (μm)	d_2 (μm^3)	d_4 (μm^5)	d_6 (μm^7)	rms (nm)	Yield strength Y (GPa)
Manual procedure:							
3	3	4	1.7	10	0.021	0.68	7.02
10	10	7.8	10	40	0.9	0.81	7.03
50 (a)	50	22	130	190	300	0.87	7.14
Intentional modification of parameters:							
50 (b)	50	24	100	210	320	0.75	7.11
50 (c)	50	40	70	90	3000	1.03	7.25
50 (d)	50	40	70	90	infinity	0.92	7.18
Tentative objective procedure:							
3 (*)	3	9	0.82	0.14	0.85	0.43	6.81
10 (*)	10	14	4.77	4.37	1.87	0.53	7.10
50 (*)	50	20	120	148	733	1.13	7.05

Rms, root mean square deviation.

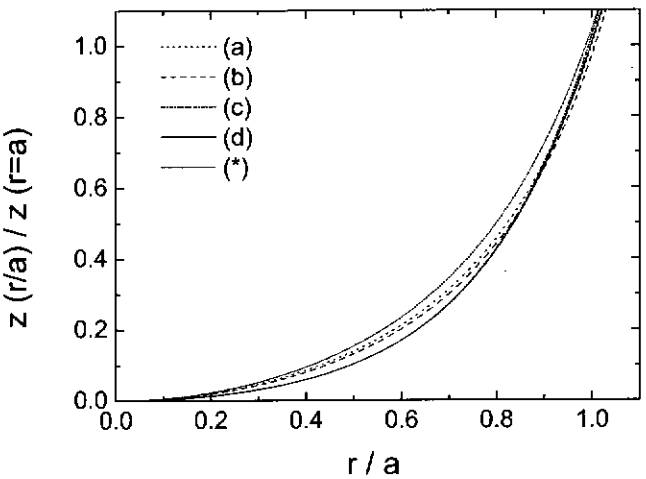

FIG. 2. Shape of the five effective indenters investigated in case of a maximum load of 50 mN [data sets 50 (a)–50 (d) and 50 (*), compare Table II]. The shape has been normalized with respect to the contact radius a and the $z(a)$.

load of 50 mN [data sets 50 (a)–50 (d) and 50 (*)]. These shapes are relatively close to each other, despite the seemingly strong variations in the d_i parameters by factors of about 2 (in case of d_0, d_2, d_4) or 10 and more for d_6. Thus, these five different parameter sets $\{d_0,d_2,d_4,d_6\}$ correspond to similar effectively shaped indenters and, therefore, deliver yield strength values that vary relatively little.

The previous results let us conclude that the manual fit—notwithstanding its subjective aspects—is obviously able to provide reliable values of the yield strength. Nevertheless, it would be a big advantage to exclude subjective influences completely. As a first tentative approach to obtain the set of d_i parameters in an objective manner, i.e., in a way that is independent of the specific person doing the analysis, we have performed the following procedure. First, a preliminary set of d_i parameters was calculated automatically using the so-called X-Fit option of the software FilmDoctor.[24] Then, the coefficient d_0 was varied such that the rms deviation was minimized. No changes in the other parameters (d_2, d_4, and d_6) were done. This simple and fast procedure delivered reliable results [compare Table II, data sets 3 (*), 10 (*), and 50 (*)] with yield strength values between 6.8 and 7.1 GPa. In two cases [parameter sets 3 (*) and 10 (*)], the rms deviations between measured and simulated curves were even smaller than in case of the sets obtained before.

C. Stress fields due to the effectively shaped indenter

In this section we will analyze the consequences of the specific shape of the effective indenter (as described by the sets of d_i parameters given in Table II) on the distributions of the contact stress (i.e., the normal stress at the surface) as well as the elastic von Mises stress within the sample volume. With the known set of d_i coefficients, the set of c_i coefficients can be calculated, which determines the distribution of the contact stress corresponding to Eq. (14). In Fig. 3, the contact stress in dependence on r/a is shown for all manual fits, i.e., the data sets 3, 10, and 50 (a) in Table II. For comparison, the contact pressure distribution of the Hertzian form was also plotted and showed a qualitatively different character. Considering the m-value of about 1.23 for all loads it is plausible that the pressure distributions are practically load independent. This distribution resembles a superposition of pressure distributions due to a flat punch and an indenter of parabolic shape. Its maximum is situated close to the contact edge and the distribution is relatively flat.

Figure 4 shows the contact stress distribution due to the effective indenter acting elastically at maximum load for the four data sets 50 (a)–50 (d). We can see that the distribution changed very little when d_0 is increased by about 10% and the other d_i parameters adjusted accordingly [50 (a) versus 50 (b)]. The same is the case for the substitution of d_6 = 3000 by infinity [50 (c) versus 50 (d)]. Between these two "pairs of similar

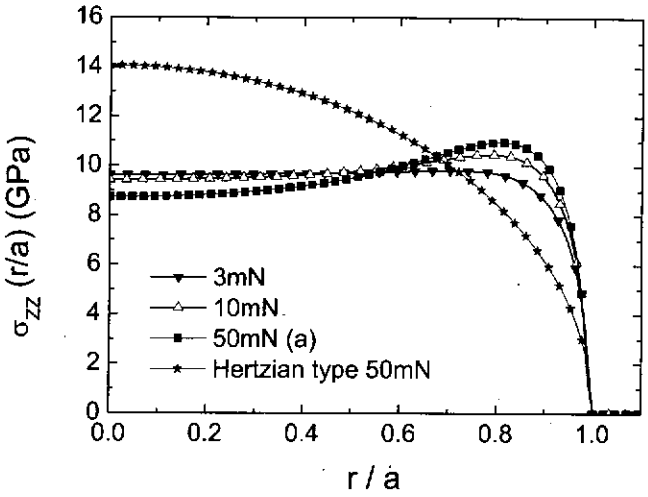

FIG. 3. Contact stress due to the elastic stresses of the effective indenter in dependence on *r/a* for all manual fits, i.e., the data sets 3, 10, and 50 (a) in Table II. For comparison, the contact pressure distribution of the Hertzian form was also plotted with a qualitatively different character.

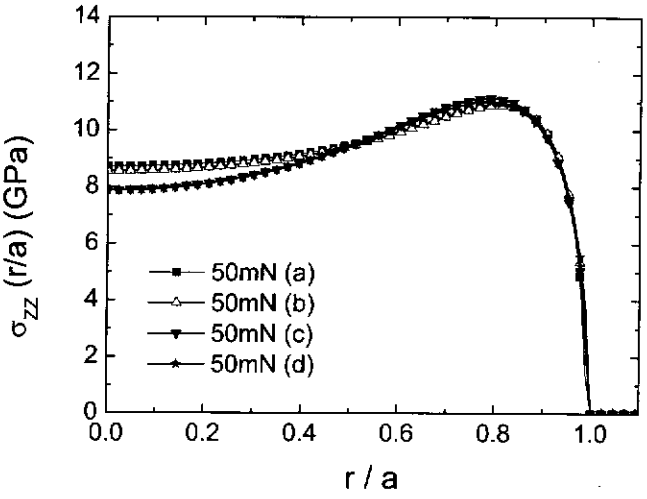

FIG. 4. Contact stress distribution due to the elastic stresses of the effective indenter for the four data sets 50 (a)–50 (d) (see Table II).

distributions" exists a certain difference particularly in the middle of the contact area which, however, has only a very limited effect on the yield strength obtained as discussed previously.

In Figs. 5 and 6, the distribution of the elastic von Mises stress at maximum load for data sets 50 (a) (manual fit) and 50 (*) (objective procedure) are given. In both cases the maximum of the elastic von Mises stress is situated outside the axis of rotational symmetry, however, at different radial and height (z) positions: For data set 50 (a) the radial position (1.08 μm) is ~20% bigger than for set 50 (*) (0.90 μm), whereas the z-position for 50 (a) (0.28 μm) is only 62% of that for 50 (*), which is 0.45 μm. In contrast to these large differences the values of the maxima are similar (7.14 and 7.05 GPa,

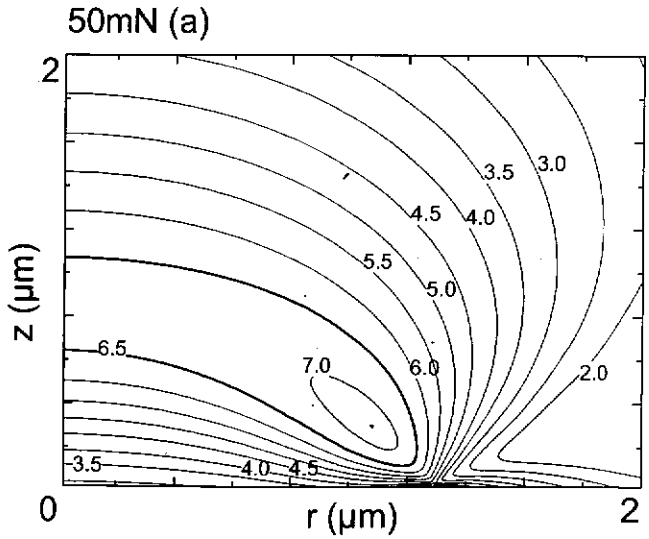

FIG. 5. Distribution of the elastic von Mises stress at maximum load for data set 50 (a) (manual fit). The maximum of the elastic von Mises stress is situated at the radial position of 1.08 μm and the z-position of 0.28 μm, the corresponding value of the maximum is 7.14 GPa.

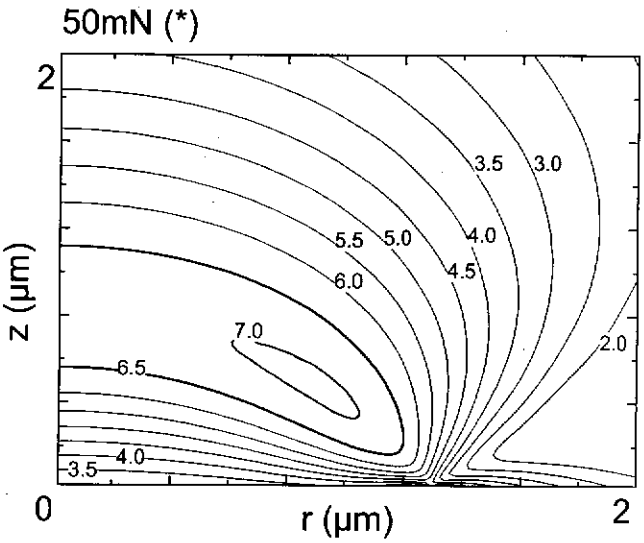

FIG. 6. Distribution of the elastic von Mises stress at maximum load for 50 (*) (objective procedure). The maximum of the von Mises stress is situated at the radial position of 0.90 μm and the z-position of 0.45 μm; the corresponding value of the maximum is 7.05 GPa.

respectively, compare Table II), and the distribution as a whole is also practically the same as can be seen by the contour lines for the stress values $\leq$ 6.5 GPa.

IV. APPLICATION OF THE EFFECTIVE INDENTER CONCEPT TO DATA OBTAINED BY FINITE ELEMENT SIMULATIONS

A. Finite element model

Elastic–plastic indentation was simulated using the commercial finite element code ANSYS (Canonsburg, PA). The contact problem has been modeled using an

axisymmetric setup, where the indenter was modeled as a rigid cone with an angle of the indenter face to the specimen surface of $\gamma = 19.7°$ corresponding to the average value of this angle in case of a pyramidal Berkovich indenter. The specimen was modeled as a large cylinder $H = 100$ μm in height and $W = 100$ μm in radius, which was represented by ~25,000 four-node axisymmetric elements. The simulation was performed up to an indentation depth of $h_{max} = 0.4$ μm. According to this, the dimensions of the specimen were found to be large enough to approximate a semi-infinite body. A symmetry boundary condition (roller b.c.) has been applied along the centerline, no displacement was allowed at the bottom surface, the outer surface was modeled as free, and the contact between the indenter and the specimen surface was considered to be frictionless. The mesh was chosen to be very fine in the region of the contact, and the element size was increased progressively with increasing distance from the contact. A large strain formulation has been used with the material behavior of a von Mises solid, which is shown in Fig. 7. The material parameters used in the simulation were those of fused silica (yield strength $Y = 7$ GPa, Young's modulus of $E = 72$ GPa, and Poisson's ratio $\nu = 0.17$). The aim of this finite element simulation was not to match exactly the experimental load–depth curves and to reevaluate the experimental results obtained. It was rather used as a parallel independent computational experiment to study the concept of the effective indenter in the form of the EHA for the determination of yield strength. Additionally, the loading and unloading of the simulated load–depth curve have been analyzed using empirical power-law fits, where the exponents contain information about the shape of the contacting bodies and the resulting pressure distributions. For the loading part, an empirical relation of $P \propto h^{\kappa}$ has frequently been suitable to model the elastic–plastic load–depth curves of Berkovich indenters onto a flat half-space.[27,28] In this case, an exponent κ of about 2 was obtained. The unloading curve were analyzed by means of the power-law fit according to Eq. (1), where the exponent m provides information about the shape of the effective indenter as previously mentioned.

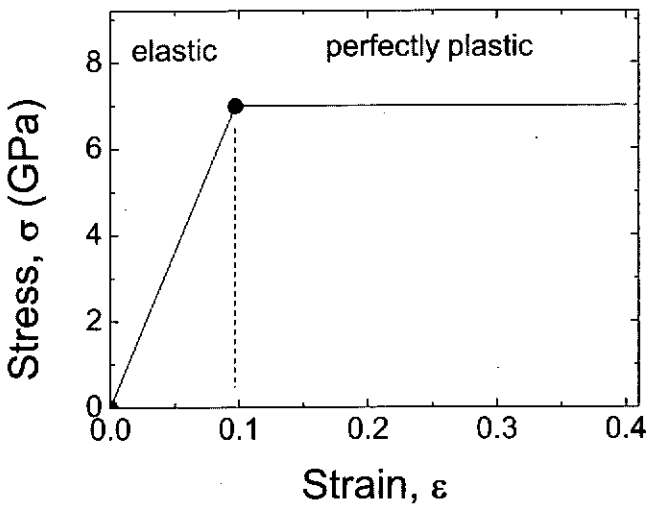

FIG. 7. Material constitutive law of a von Mises solid used for the finite element simulation with a yield strength $Y = 7$ GPa, Young's modulus of $E = 72$ GPa, and Poisson's ratio $\nu = 0.17$.

B. Simulation results

The load–depth curve obtained by the elastic–plastic finite element simulation of the material chosen is shown in Fig. 8. With a maximum load of $P_{max} = 22$ mN, the elastic recovery obtained during unloading was about $h_s = 225$ nm and the final depth obtained was about $h_f = 175$ nm. The hardness value observed in the finite element simulation was estimated to be 10.4 GPa.

The analysis of the loading and unloading curves revealed that the loading curve during elastic–plastic contact was well described by the power-law fit given by $P \propto h^{\kappa}$ with an exponent of $\kappa = 1.96$ (Fig. 8), which is in agreement with exponents obtained from experimental data mentioned previously and indicates a proper elastic–plastic deformation of the material. The unloading curve is distinctly curved and can be approximated by the power-law fit $P = \alpha (h - h_f)^m$ with an exponent $m = 1.31$ (compare Fig. 8). This value is similar to the value of 1.23 obtained from our experiments (compare Table II) and again represents an indenter shape corresponding to a flat punch superposed with a quadratic parabola. The exponent m was used to calculate the exponent n in Eq. (11) with a resulting value of $n = 3.2$. The analysis of the unloading part of the load–depth

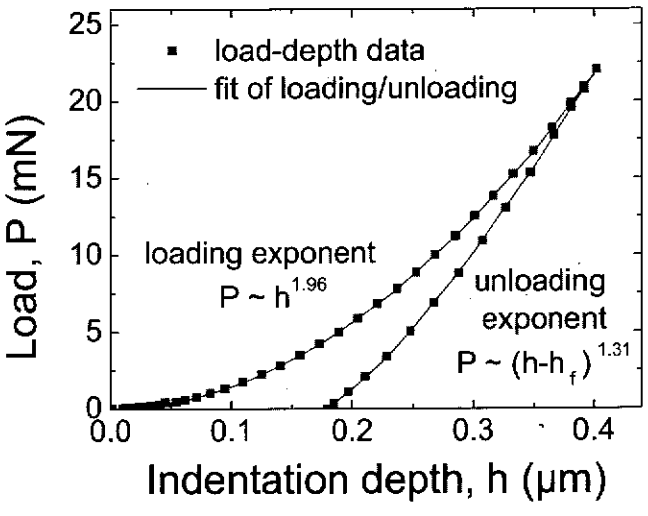

FIG. 8. Simulated load–depth curve obtained by the elastic–plastic finite element simulation. The loading curve was well described by the power-law fit corresponding to $P \propto h^{\kappa}$ with an exponent of $\kappa = 1.96$, and the unloading curve is distinctly curved and was approximated by the power-law fit $P = \alpha (h - h_f)^m$ with an exponent $m = 1.31$.

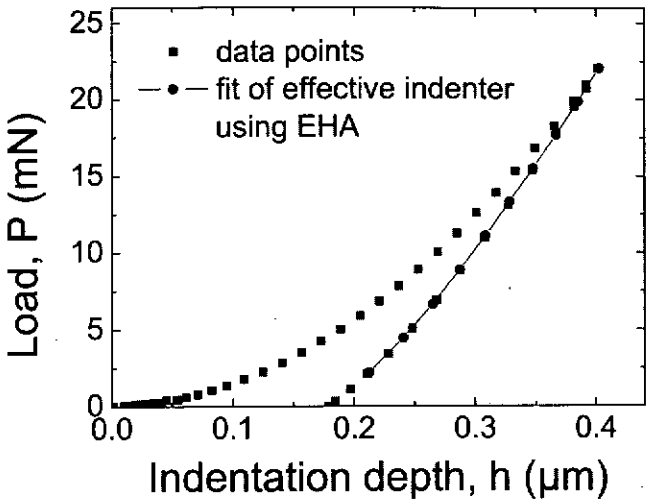

FIG. 9. Fit of the simulated unloading curve by means of the EHA showing an excellent description of the data points.

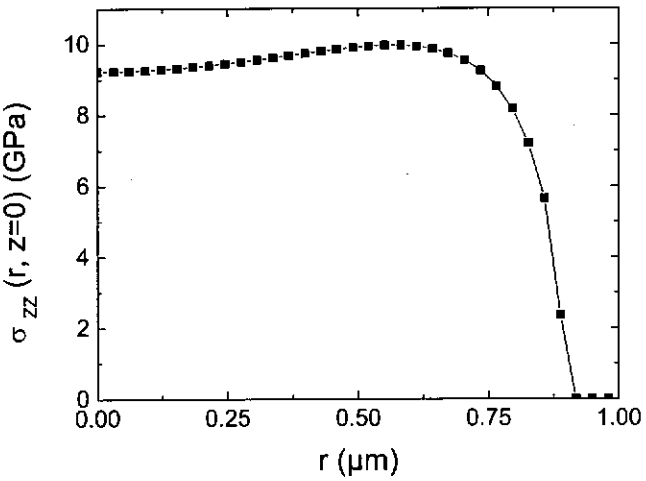

FIG. 10. Contact stress distribution due to the elastic stresses of the effective indenter obtained by the EHA.

curve was performed by means of the EHA in the same way as for the experimental curves (compare Sec. III. B) and the following coefficients were obtained: d_0 = 15 μm, d_2 = 20 μm^3, d_4 = 40 μm^5, and d_6 = 250 μm^7. From these d_i coefficients, a similar conclusion, as for the experimental data, was drawn that in addition to the parabolic term r^2 the higher order terms of r^i also influenced the resulting shape of the effective indenter, which is in agreement with the value of the exponent m = 1.31.

As Fig. 9 shows, these d_i coefficients provide an excellent description of the unloading curve calculated by the finite element method. Then, from the resulting d_i coefficients, the c_i coefficients were calculated, which determined the shape of the contact stress distribution due to the elastic indenter stresses of the effective indenter, as shown in Fig. 10. It can be seen that this stress distribution is relatively flat over the contact region and

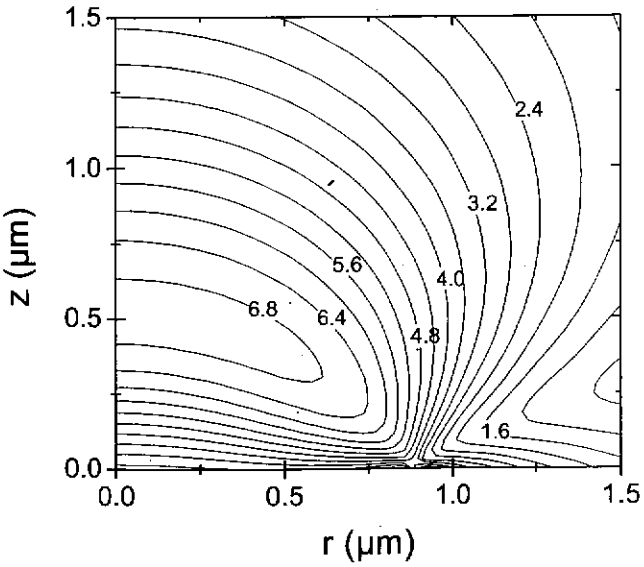

FIG. 11. Elastic von Mises stress distribution due to the effective indenter obtained from the simulated load–depth curve (Fig. 9) delivering a maximum of σ_M = 6.95 GPa (yield strength) in excellent agreement with the yield strength of 7.0 GPa used as input for fused silica in the finite element model.

shows a slight increase toward the contact edge. This is plausible because of the contribution of r^i terms of higher order, and is in accordance with the unloading exponent m = 1.31. Moreover, the type of resulting pressure distribution obtained in this case is similar to the results of the experiments of Sec. III. B.

Finally, with the known c_i coefficients, the complete elastic stress field within the material was computed. Following the already provided arguments (compare Sec. II. D), the spatial maximum of the elastic von Mises stress distribution was used as a measure of the yield strength of materials. The corresponding von Mises stress distribution is shown in Fig. 11, and, indeed, the obtained value of σ_M = 6.95 GPa showed an excellent agreement to the yield strength of 7 GPa used as input for fused silica in the finite element model.

As mentioned previously, the m-value of 1.31 for the simulated load–depth curves was somewhat larger than the m = 1.23 for the experimental data, thus influencing the shape of the contact stress distributions and the elastic von Mises stress field. These differences are most likely an expression of the fact that the real deformation behavior of fused silica is more complex than it was considered in the simulation. However, the finite element simulation has shown that the input value of yield strength is in good agreement with the value obtained by the EHA, thus supporting this approach.

V. CONCLUSIONS

Fused silica samples have been investigated by nanoindentation with a Berkovich indenter applying data analysis

on the basis of the "effectively shaped indenter" concept. As expected, the investigations have shown that the hardness was practically independent of the maximum load during the measurement. Moreover, the yield strength determined using the method of the effectively shaped indenter also proved to be independent of the load.

In the effectively shaped indenter concept, self similarity in an indentation process is reflected in the fact that for an increased maximum indentation load an "effective indenter" is obtained that increased in size but is maintaining its shape. The latter is shown in the fact that the exponent m corresponding to Eq. (1) and the contact pressure distribution due to the elastic stresses of the effective indenter (compare Fig. 3) are practically independent of the load. The increase in size of the effective indenter is such that the mean contact pressure, which represents the hardness, stays constant when the maximum load is changed. Eventually, the practically load-independent shape of the contact pressure distribution, together with its constant average value, creates such a distribution of the elastic von Mises stress in the sample that for varying maximum load one and the same yield strength value is obtained.

The shape of the effective indenter was described in terms of a parameter set $\{d_0,d_2,d_4,d_6\}$ with the parameters d_i being determined by means of the manual fit described in Sec. III. B. Determination of the yield strength from the effective indenter obtained this way delivered practically one and the same value of (7.1 ± 0.1) GPa for all loads investigated. Even intentional large modifications of the d_0 value by 10% and 100%, respectively, followed by a readjustment of the other parameters resulted only in a slight shift of the yield strength values toward (7.2 ± 0.1) GPa. This lets one conclude that the manual fit, despite the fact that it includes a certain level of arbitrariness, is obviously able to provide reliable values of the yield strength. Nevertheless, the complete avoidance of subjective influences would be a big advantage. As a first step, we have applied a preliminary objective procedure (compare Sec. III. B), which delivered reliable values of the yield strength in the range of (6.8 to 7.1) GPa in a fast and easy way.

Finite element simulation of elastic–plastic indentation of a rigid cone into a von Mises solid having the material parameters of fused silica, including yield strength of 7.0 GPa, has been performed. The simulated unloading curve was analyzed using the method of the effectively shaped indenter and the d_i parameters corresponding to the EHA have been determined. From that the yield strength was determined analogously to the case of the experimental curve and a value of 6.95 GPa was obtained. This result again supports the reliability of the effectively shaped indenter concept.

Finally, it should be mentioned that the material used in this work seemed to be particularly well suited for the application of the method. Although several other materials have been successfully investigated using the effectively shaped indenter concept in the form of the EHA,[4,7] a detailed investigation of the limits of applicability of the method remains to be done. Further experimental and numerical studies on materials of a wide range of varying stress–strain characteristics and varying ratios of E/Y are planned for the future.

ACKNOWLEDGMENTS

The authors thank the anonymous referees for valuable suggestions for the present study. In addition, the financial support from the German Research Foundation (DFG) is highly acknowledged, as well as valuable discussions with J. Mehner (Chemnitz University of Technology, Germany).

REFERENCES

1. W.C. Oliver and G.M. Pharr: Measurement of hardness and elastic modulus by instrumented indentation: Advances in understanding and refinements to methodology. *J. Mater. Res.* **19,** 3 (2004).
2. G.M. Pharr and A. Bolshakov: Understanding nanoindentation unloading curves. *J. Mater. Res.* **17,** 2660 (2002).
3. I.N. Sneddon: The relation between load and penetration in the axisymmetric Boussinesq problem for a punch of arbitrary profile. *Int. J. Eng. Sci.* **3,** 47 (1965).
4. N. Schwarzer: Elastic surface deformation due to indenters with arbitrary symmetry of revolution. *J. Phys. D: Appl. Phys.* **37,** 2761 (2004).
5. N. Schwarzer and G.M. Pharr: On the evaluation of stresses during nanoindentation with sharp indenters. *Thin Solid Films* **469/470,** 194 (2004).
6. N. Schwarzer: Arbitrary load distribution on a layered half space. *ASME J. Tribol.* **122,** 672 (2000).
7. N. Schwarzer, T. Chudoba, and F. Richter: Investigation of ultra thin coatings using nanoindentation. *Surf. Coat. Technol.* **200,** 5566 (2006).
8. W.C. Oliver and G.M. Pharr: An improved technique for determining hardness and elastic modulus using load and displacement sensing indentation. *J. Mater. Res.* **7,** 1564 (1992).
9. J.L. Loubet, J.M. Georges, O. Marchesini, and G. Meille: Vickers indentation curves of magnesium oxide (MgO). *ASME J. Tribol.* **106,** 43 (1984).
10. M.F. Doerner and W.D. Nix: A method for interpreting the data from depth-sensing indentation instruments. *J. Mater. Res.* **1,** 601 (1986).
11. J.C. Hay, A. Bolshakov, and G.M. Pharr: A critical examination of the fundamental relations used in the analysis of nanoindentation data. *J. Mater. Res.* **14,** 2296 (1999).
12. J. Woirgard and J.C. Dargenton: An alternative method for penetration depth determination in nanoindentation measurements. *J. Mater. Res.* **12,** 2455 (1997).
13. H. Hertz: On the contact of elastic solids. *J. Reine Angew. Mech.* **92,** 156 (1881).
14. H. Hertz: *Hertz's Miscellaneous Papers* (Macmillan, London, 1896), p. 146.

15. V.I. Fabrikant: *Application of Potential Theory in Mechanics: A Selection of New Results* (Kluwer Academic Publishers, Dordrecht, The Netherlands, 1989).
16. T. Chudoba, N. Schwarzer, and F. Richter: New possibilities of mechanical surface characterization with spherical indenters by comparison of experimental and theoretical results. *Thin Solid Films* **355/356,** 284 (1999).
17. T. Chudoba, N. Schwarzer, and F. Richter: Determination of elastic properties of thin films by indentation measurements with a spherical indenter. *Surf. Coat. Technol.* **127,** 9 (2000).
18. T. Chudoba, M. Griepentrog, A. Dück, D. Schneider, and F. Richter: Young's modulus measurements on ultra-thin coatings. *J. Mater. Res.* **19,** 301 (2004).
19. F. Richter, M. Herrmann, F. Molnar, T. Chudoba, N. Schwarzer, M. Keunecke, K. Bewilogua, X.W. Zhang, H.G. Boyen, and P. Ziemann: Substrate influence in Young's modulus determination of thin films by indentation methods: Cubic boron nitride as an example. *Surf. Coat. Technol.* **201,** 3577 (2006).
20. T. Chudoba, N. Schwarzer, F. Richter, and U. Beck: Determination of mechanical film properties of a bilayer system due to elastic indentation measurements with a spherical indenter. *Thin Solid Films* **377/378,** 366 (2000).
21. T. Chudoba, N. Schwarzer, and F. Richter: Steps towards a mechanical modeling of layered systems. *Surf. Coat. Technol.* **154,** 140 (2002).
22. N. Schwarzer: Coating design due to analytical modelling of mechanical contact problems on multilayer systems. *Surf. Coat. Technol.* **133/134,** 397 (2000).
23. R. Puschmann, N. Schwarzer, F. Richter, S. Fruehauf, and S. E. Schulz: A usable concept for the indentation of thin porous films. *Z. Metallkd.* **96,** 1272 (2005).
24. Filmdoctor. Available at: http://www.siomec.de/filmdoctor.
25. J.S. Field and M.V. Swain: A simple predictive model for spherical indentation. *J. Mater. Res.* **8,** 297 (1993).
26. T. Chudoba and M. Griepentrog: Comparison between conventional Vickers hardness and indentation hardness obtained with different instruments. *Z. Metallkd.* **96,** 1242 (2005).
27. A.C. Fischer-Cripps: Critical review of analysis and interpretation of nanoindentation test data. *Surf. Coat. Technol.* **200,** 4153 (2006).
28. J. Malzbender and G. de With: Indentation load-displacement curve, plastic deformation, and energy. *J. Mater. Res.* **17,** 502 (2002).